APL Materials

Hole-transport comparison between solution-processed and vacuum-deposited organic semiconductors

Cite as: APL Mater. **7**, 011105 (2019); https://doi.org/10.1063/1.5058686
Submitted: 18 September 2018 . Accepted: 18 December 2018 . Published Online: 24 January 2019

Deepthi K. Mangalore, Paul W. M. Blom, and Gert-Jan A. H. Wetzelaer

Hole-transport comparison between solution-processed and vacuum-deposited organic semiconductors

Cite as: APL Mater. 7, 011105 (2019); doi: 10.1063/1.5058686
Submitted: 18 September 2018 • Accepted: 18 December 2018 •
Published Online: 24 January 2019

Deepthi K. Mangalore, Paul W. M. Blom, and Gert-Jan A. H. Wetzelaer

AFFILIATIONS

Max Planck Institute for Polymer Research, Ackermannweg 10, 55128 Mainz, Germany

ABSTRACT

Charge transport in the amorphous organic small molecules α-NPD (N,N′-di(1-naphthyl)-N,N′-diphenyl-(1,1′-biphenyl)-4,4′-diamine) and Spiro-TAD (2,2′,7,7′-tetrakis(N,N-diphenylamino)-9,9-spirobifluorene) is investigated in solution-processed films and compared to charge transport in vacuum-deposited films of the same molecule. By optimizing the solution-deposition conditions, such as solvent and concentration, equal charge-transport parameters for solution-processed and vacuum-deposited films are demonstrated. Modeling of the charge carrier transport characteristics was performed by drift-diffusion simulations. The dependence of the charge carrier mobility on temperature, carrier density, and electric field was found to be the same for vacuum deposition and solution processing. In both material processing cases, hole mobilities of 4×10^{-8} m^2 V^{-1} s^{-1} for spiro-TAD and 0.9×10^{-8} m^2 V^{-1} s^{-1} for α-NPD are obtained, demonstrating that solution processing can be a viable alternative to vacuum deposition in terms of charge transport.

The field of display technology and lighting in the last decade has been revolutionized by the discovery of organic light-emitting diodes (OLEDs) based on π-conjugated organic semiconductors.[1,2] In addition, small-molecular organic semiconductors are widely used in charge-transport layers in perovskite photovoltaic devices.[3] The opportunity presented by these technologies has driven the research to find cheaper alternatives to the traditional deposition method of layers of organic small molecules by thermal evaporation in high vacuum. The solubility of organic semiconductors in organic solvents renders them suitable for film deposition from solution, which can be scaled up to a cost-effective roll-to-roll process.[1,2] However, it is unclear whether solution-processed films of organic semiconductors can maintain the same film quality and charge-transport characteristics as compared to vacuum-deposited films. Usually, to obtain solution processability, the chemical structure of organic molecules is modified, typically by adding solubilizing side chains to the conjugated moiety.[4,5] However, these insulating sidechains also affect the charge-transport properties, complicating a direct comparison with their vacuum-deposited counterparts.

Solution-processed small-molecular charge-transport layers in OLEDs have been reported as early as two decades ago.[6] More recently, efforts have been made to systematically replace vacuum-deposited transport- and emitting-layers in OLED stacks by solution processed layers and investigating their effect on the OLED performance.[7–9] To compare the charge-transport characteristics of individual layers of solution- and vacuum-deposited small molecules, single-carrier devices have been investigated.[7,8] Dissimilar current-voltage characteristics were obtained, possibly affected by the presence of a variation in injection barrier.[7] While morphological differences have been investigated in films of spin-coated and vacuum-deposited amorphous small molecules,[10] a detailed analysis and comparison of the charge-transport properties of solution- and vacuum-deposited films of organic small molecules has not been reported to date. Additionally, the modeling of the transport characteristics from different processing conditions has not been investigated.

Here, we investigate the hole transport in solution-processed and vacuum-deposited films of the commonly

used amorphous hole-transport molecules α-NPD (N,N′-di(1-naphthyl)-N,N′-diphenyl-(1,1′-biphenyl)-4,4′-diamine) and spiro-TAD (2,2′,7,7′-tetrakis(N,N-diphenylamino)-9,9-spirobifluorene) by space-charge-limited current measurements in single-carrier devices with Ohmic hole contacts and verify it by numerical modeling. After optimizing the solution process, smooth and uniform films with near identical charge-transport properties are obtained as compared to vacuum-deposited films of the same molecule.

The two investigated hole-transport materials, spiro-TAD and α-NPD (both sublimed grade), were purchased from Luminescence Technology Corp. and Sigma-Aldrich, respectively, and used as received. The hole-only devices were fabricated in the sandwich geometry consisting of a bottom electrode, a small molecule thin film, and a top electrode.[11,12] Glass substrates pre-patterned with indium-tin oxide were first cleaned with neutral soap and then rinsed with deionized water, followed by sonication in acetone and isopropanol, and UV-ozone treatment. Next, a 55 nm thick film of poly(3,4-ethylenedioxythiophene):polystyrene sulfonate (PEDOT:PSS; Clevios P VP Al4083, Heraeus) was spin-coated from an aqueous dispersion and then annealed at 140 °C for 10 min in air. Subsequently, organic thin films of α-NPD or spiro-TAD were deposited by either spin coating or conventional vacuum-deposition. For spin coating, solutions of different concentrations in chloroform, chlorobenzene, or toluene were spin cast in nitrogen atmosphere, followed by annealing for 10 min at 50 °C. Alternatively, vacuum deposition was carried out at a deposition rate of 1-2 Å/s at a base pressure of 1×10^{-7} mbar. For Ohmic-contact formation, a 5 nm layer of tris(4-carbazoyl-9-ylphenyl)amine (TCTA) vacuum-deposited between the hole-transport layer and the vacuum-deposited MoO_3 (10 nm)/Al (100 nm) top electrode.[13] The current density-voltage (J-V) characteristics were recorded with a Keithley 2400 source meter. All measurements were carried out in nitrogen atmosphere. The thickness of the films was measured using a Bruker Dektak XT profilometer.

In the solution process, spiro-TAD was deposited using three different solvents. The current density-voltage characteristics of the hole-only devices were then compared to a thermally evaporated control device, as shown in Fig. 1. Similar current densities to the control device were obtained for the solution-processed films when using chlorobenzene or toluene as a solvent. As the current density scales directly with the hole mobility in a space-charge-limited device, the almost identical J-V characteristics indicate that hole transport in these solution-processed films is equal to the hole transport in the vacuum-deposited film. On the other hand, the current in the chloroform-processed spiro-TAD device is a factor of 4 lower, showing that the used solvent can influence the hole transport. A more prominent effect of the solvent is observed for α-NPD. α-NPD was found to be less soluble and more difficult to process from solution. However, for chlorobenzene-processed films, the measured hole current was found to approach the current of the vacuum-deposited control device, as shown in Fig. 2.

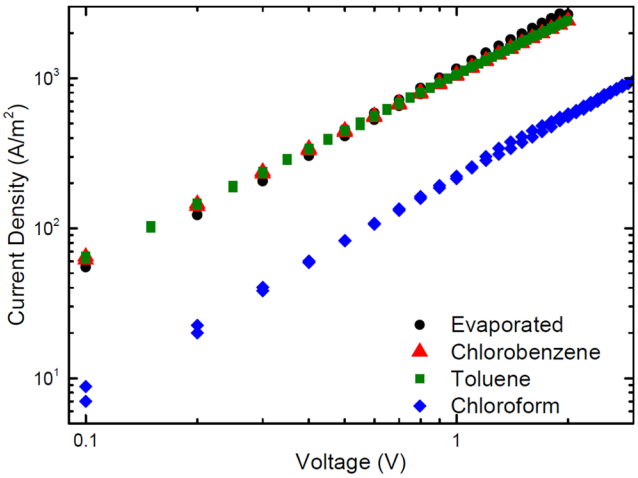

FIG. 1. Experimental current density-voltage characteristics of hole-only devices with a spiro-TAD layer thickness of 100 nm. The solution-processed films spin-cast from chlorobenzene (red triangles), toluene (green squares), and chloroform (blue diamonds) are compared to a thermally evaporated (black circles) reference device.

The results above demonstrate that solution-processed films of spiro-TAD and α-NPD can have similar hole transport to their vacuum-deposited counterparts at room temperature. To investigate the charge transport in more detail, temperature-dependent J-V characteristics were measured, which were modeled with one-dimensional drift-diffusion simulations,[14] from which the hole mobilities were evaluated. The charge-carrier mobility in disordered organic semiconductors is dependent on temperature, charge-carrier density, and electric field.[14,15] For hopping transport between states having a Gaussian distribution in energy, the mobility

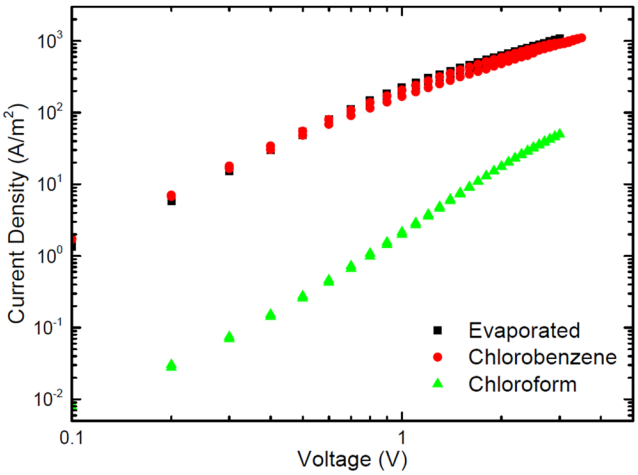

FIG. 2. Experimental current density-voltage characteristics of hole-only devices with an α-NPD layer with a thickness of ~100 nm. Thermally evaporated devices (black squares) are compared to solution-cast films from different solvents: chloroform (green triangles) and chlorobenzene (red circles).

has been described by the extended Gaussian disorder model (EGDM).[14]

In this model, the charge transport is characterized by the width of the density-of-states distribution σ, the lattice constant a, and a mobility prefactor μ_∞. With increasing energetic disorder, the mobility becomes increasingly dependent on temperature, according to[14]

$$\mu_0(T) = \mu_\infty c_1 \exp\left[-c_2\left(\frac{\sigma}{kT}\right)^2\right], \quad (1)$$

where $c_1 = 1.8 \times 10^{-9}$ and $c_2 = 0.42$ are given by the EDGM, k is the Boltzmann constant, and T is the temperature. Here, $\mu_0(T)$ denotes the temperature-dependent mobility in the limit of vanishing carrier density and electric field. Apart from the influence of σ on the temperature dependence, also the density dependence of the mobility becomes stronger for increased energetic disorder. The lattice constant a mostly influences the field dependence of the mobility, with a stronger field dependence for larger lattice constants.

The constants c_1 and c_2 are obtained in Ref. 14 from the parametrization of the solution of the master equation for hopping transport on a cubic lattice of sites Gaussianly distributed in energy. Even though these constants are obtained for a lattice model, it has been shown that for simulated morphologies of α-NPD, a constant $c_2 = 0.41$ is obtained, very similar to the constant in the EGDM, justifying its applicability.[16] The constant c_1 can be included in the mobility prefactor. The mobility prefactor μ_∞ is a temperature-independent parameter that only influences the magnitude of the mobility and is used as a fit parameter, next to the density-of-states distribution and the lattice constant.

The experimental temperature-dependent J-V characteristics were modeled with drift-diffusion simulations incorporating the EGDM mobility function, as displayed in Fig. 3. The experimental data can be consistently described for both solution-processed and thermally evaporated films, with the same set of parameters. We find that the energetic disorder is 0.09 eV in both thermally evaporated and optimized solution-processed devices. The used lattice constant was 1.1 nm in both cases. The mobility at 295 K at zero electric field and carrier density was found to be 4×10^{-8} m^2/V s for both solution- and vacuum-deposited films. This value is also consistent with time-of-flight measurements on thermally evaporated spiro-TAD.[17] The temperature dependent J-V measurements of a hole-only device with a different spiro-TAD thickness (100 nm) can also be modeled with the same parameters and fits with the EGDM (Fig. S1 of the supplementary material). The results from the two different thicknesses show that equal mobilities can be obtained irrespective of the device thickness.

For α-NPD, the hole mobility in the chlorobenzene-processed film amounted to 0.9×10^{-8} m^2/V s, approaching the value for the vacuum-deposited reference. The energetic disorder was found to be 0.09 eV in both cases, similar to previously reported values.[11,16] The similar mobility and disorder values obtained for solution-processed and vacuum-deposited films of α-NPD and spiro-TAD show that charge transport can be equally good for both deposition methods. The lower mobility in chloroform-cast films may arise from increased energetic disorder in these films. This hypothesis is supported by the increased temperature dependence of the J-V characteristics in chloroform-cast films compared to toluene-cast films (see the supplementary material). When modeled using the EGDM, we find that the disorder parameter in chloroform-cast films is 0.12 eV, which is larger than the energetic disorder obtained for toluene-cast and vacuum-deposited films (0.09 eV).

In order to compare the surface morphology, spin-coated and vacuum-deposited thin films were prepared on glass-ITO substrates. The spin cast films were deposited in a nitrogen atmosphere from solutions of spiro-TAD in

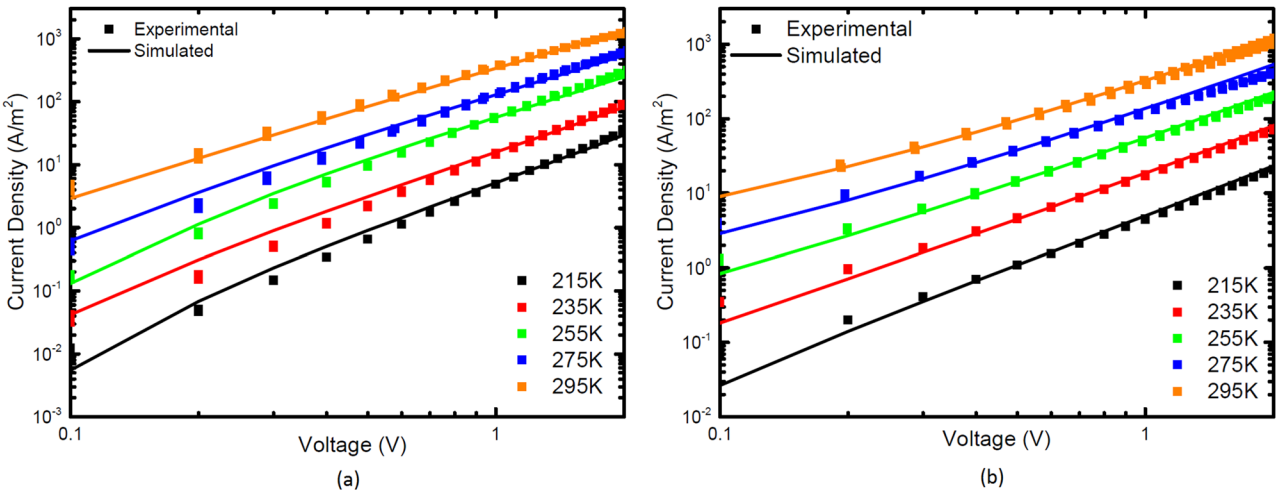

FIG. 3. Temperature-dependent experimental (symbols) and simulated (lines) current density-voltage characteristics of spiro-TAD hole-only devices with a layer thickness of 180 nm, solution-processed from toluene (a) and vacuum-deposited (b).

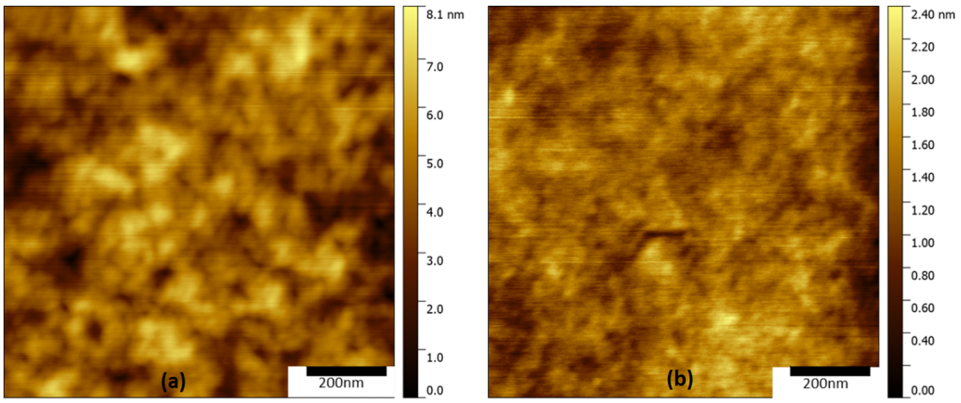

FIG. 4. AFM topography (scale bar 200 nm) of vacuum-deposited spiro-TAD films (a) and spiro-TAD spin-cast from toluene solution (b). The measurement area size is $1 \times 1\ \mu m^2$.

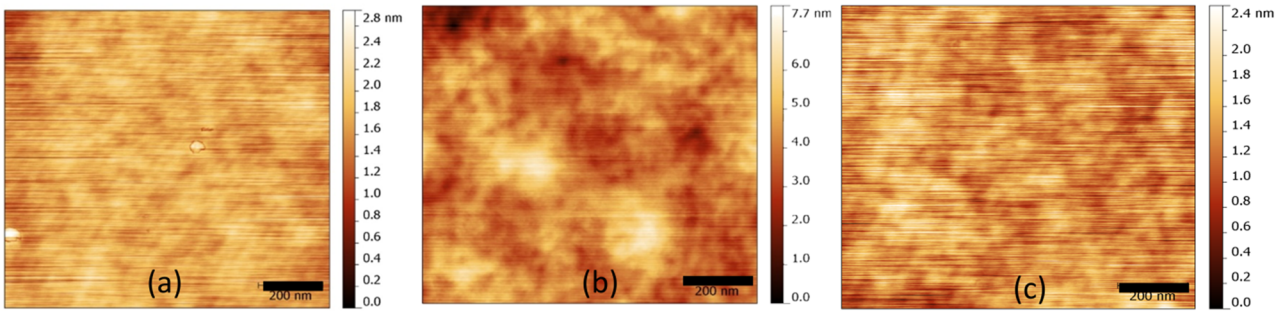

FIG. 5. Atomic force micrographs (scale bar 200 nm) of α-NPD films processed by (a) thermal evaporation and from solutions of (b) chloroform and (c) chlorobenzene. Films processed using chlorobenzene as a solvent are found to have surface roughness comparable to the vacuum-deposited films (2.4 and 2.8 nm). The film processed using chloroform is found to have higher roughness (7.7 nm). The measurement area size used is $1 \times 1\ \mu m^2$.

chlorobenzene and toluene. Figure 4 shows the atomic-force microscopy (AFM) images of the vacuum-deposited and spin-coated thin films of spiro-TAD on the ITO substrates. The root mean square (RMS) roughness values of the surface of films obtained by thermal evaporation, chlorobenzene deposition, and toluene deposition were 8.1 nm, 2.4 nm, and 2.1 nm, respectively. Hence, the spin-coated spiro-TAD films are even smoother in comparison with the thermally evaporated films. For α-NPD, the RMS roughness was determined to be 2.8 nm for the thermally evaporated film and 2.4 nm for the chlorobenzene-cast film. The chloroform-cast film had an RMS roughness of 7.7 nm. As expected for amorphous materials, the AFM topography images do not show any distinct features (Fig. 5).

In summary, hole transport was studied in films of the small molecules of spiro-TAD and α-NPD deposited using two different methods: solution processing and thermal evaporation. Even though these molecules are originally designed for vacuum deposition, the obtained hole mobility can reach equal values when these materials are deposited from solution. Numerical simulations of the temperature-dependent hole transport using the EGDM resulted in equal values for the energetic disorder, amounting to 0.09 eV for both materials and deposition processes. The numerical simulations are found to be in excellent agreement with the experimental transport characteristics. AFM characterization indicated that the solution-processed films were smooth and uniform. Our comprehensive experimental and numerical study of the transport properties for different deposition conditions shows that solution processing can be tailored to be a viable alternative to vacuum deposition for charge-transport layers in optoelectronic devices.

See supplementary material for additional hole-transport data and simulations.

The authors thank C. Bauer, M. Beuchel, H.-J. Guttmann, F. Keller, and V. Maus for technical support. This project has received funding from the European Union Horizon 2020 research and innovation programme under Grant Agreement No. 646176 (EXTMOS).

REFERENCES

[1] R.-P. Xu, Y.-Q. Li, and J.-X. Tang, "Recent advances in flexible organic light-emitting diodes," J. Mater. Chem. C **4**, 9116–9142 (2016).
[2] H.-W. Chen, J.-H. Lee, B.-Y. Lin, S. Chen, and S.-T. Wu, "Liquid crystal display and organic light-emitting diode display: Present status and future perspectives," Light: Sci. Appl. **7**, 17168 (2018).
[3] R. A. Belisle, P. Jain, R. Prasanna, T. Leijtens, and M. D. McGehee, "Minimal effect of the hole-transport material ionization potential on the open-circuit voltage of perovskite solar cells," ACS Energy Lett. **1**, 556–560 (2016).

[4]K. S. Yook and J. Y. Lee, "Small molecule host materials for solution processed phosphorescent organic light-emitting diodes," Adv. Mater. **26**, 4218–4233 (2014).
[5]L. Duan *et al.*, "Solution processable small molecules for organic light-emitting diodes," J. Mater. Chem. **20**, 6392–6407 (2010).
[6]J. Salbeck, N. Yu, J. Bauer, F. Weissörtel, and H. Bestgen, "Low molecular organic glasses for blue electroluminescence," Synth. Met. **91**, 209–215 (1997).
[7]T.-W. Lee *et al.*, "Characteristics of solution-processed small-molecule organic films and light-emitting diodes compared with their vacuum-deposited counterparts," Adv. Funct. Mater. **19**, 1625–1630 (2009).
[8]S. Feng *et al.*, "A comparison study of the organic small molecular thin films prepared by solution process and vacuum deposition: Roughness, hydrophilicity, absorption, photoluminescence, density, mobility, and electroluminescence," J. Phys. Chem. C **115**, 14278–14284 (2011).
[9]G.-J. A. H. Wetzelaer *et al.*, "Combined thermal evaporated and solution processed organic light emitting diodes," Org. Electron. **12**, 1644–1648 (2011).
[10]M. Shibata, Y. Sakai, and D. Yokoyama, "Advantages and disadvantages of vacuum-deposited and spin-coated amorphous organic semiconductor films for organic light-emitting diodes," J. Mater. Chem. C **3**, 11178–11191 (2015).
[11]R. Rohloff, N. B. Kotadiya, N. I. Crăciun, P. W. M. Blom, and G. A. H. Wetzelaer, "Electron and hole transport in the organic small molecule α-NPD," Appl. Phys. Lett. **110**, 073301 (2017).
[12]A. Kunz, P. W. M. Blom, and J. J. Michels, "Charge carrier trapping controlled by polymer blend phase dynamics," J. Mater. Chem. C **5**, 3042–3048 (2017).
[13]N. B. Kotadiya *et al.*, "Universal strategy for Ohmic hole injection into organic semiconductors with high ionization energies," Nat. Mater. **17**, 329–334 (2018).
[14]W. F. Pasveer *et al.*, "Unified description of charge-carrier mobilities in disordered semiconducting polymers," Phys. Rev. Lett. **94**, 206601 (2005).
[15]L. J. A. Koster, E. C. P. Smits, V. D. Mihailetchi, and P. W. M. Blom, "Device model for the operation of polymer/fullerene bulk heterojunction solar cells," Phys. Rev. B **72**, 085205 (2005).
[16]A. Massé *et al.*, "*Ab initio* charge-carrier mobility model for amorphous molecular semiconductors," Phys. Rev. B **93**, 195209 (2016).
[17]T. P. I. Saragi, T. Spehr, A. Siebert, T. Fuhrmann-Lieker, and J. Salbeck, "Spiro compounds for organic optoelectronics," Chem. Rev. **107**, 1011–1065 (2007).